Engineering Science and Military Technologies
Volume (4) - Issue (1) - Mar 2020

ISSN: 2357- 0954
DOI: 10.21608/ejmtc.2020.42951.1151

Blur removal in QR code images using directional aperture filter

Original Article

Tarek A. Mahmoud

Department of Computer Engineering, Military Technical College, Cairo, Egypt

Keywords:
Aperture filter, gradient edge direction, image sharpening, QR code image.

Corresponding Author:
Tarek A. Mahmoud, Department of Computer Engineering, Military Technical College, Cairo, Egypt, **Tel:** 01114493493, **Email:** t.mahmoud@mtc.edu.eg

Abstract
Quick Response (QR) bar code is an extensively utilized matrix 2D bar code. Consumers are becoming familiar with acquiring information via handheld and wearable devices because of the wide-expansion of wireless network infrastructures. QR code is considered as a container filled with information whereby smart devices can directly capture and decode this information and at high speed. A preprocessing system has been proposed in this paper for enhancing QR code images suffering from low-quality. This paper introduces a deblurring module which particularly characterized by robust and real time operation which is an appropriate solution for the challenging introduced problem. This paper focuses on sharpening out of focus and motion blur QR code images by using a proposed aperture filter design. The most important reasons for these problems are because of lens imperfection, an out of focus scanning device or camera movement during the capturing process. The key point of the proposed design is that the gradient edge directions are utilized in indexing the patterns instead of the intensity of the pixel under test. The proposed technique provides useful innovation as an approach to QR code image sharpening to increasing consumer satisfaction. Finally, the significant improvement of the proposed algorithm has been indicated by means of a number of applied experiments followed by statistical analysis. This study proved that the proposed method outperforms many other sharpener type filters in both preserving of edges and minimizing distortion of signals.

I. INTRODUCTION

In the last few years, QR codes have attracted the commercial community due to their storage capabilities in hosting high capacity of information. Thus, QR codes beneficially replace the one dimensional bar codes in a number of applications. As well as being decoded in high speed, QR codes are widely utilized in a number of commercial applications. Furthermore, since bar codes can be easily captured by recently handheld devices on their screens with appropriate resolution to correctly decode it, a lot of consumer applications can utilize QR codes with several sizes in different scenarios. The following scenarios are examples, but not limited to, such as: scanning codes for shopping or product comparison, retailer loyalty cards, checking electronic tickets, delivering parcels and identification systems[1]. Also, QR codes are found in magazines, on postcards, on signs, on buses, and other consumer advertisements. Moreover, "virtual store" is a recent approach for using QR codes and is currently expanding globally. A lot of companies have nominated the virtual store concept[2].

The goal of QR codes is achieving convenience applications for handheld and wearable device consumers. People can use cameras of the smart devices to capture QR code, and then the hyperlink corresponding to the QR code can be accessed immediately[3]. QR code needs no additional hardware but only depends on its visual appearance to be decoded. The information transfer of the QR code is considerably of low cost with respect to other technologies that need specific hardware requirements[4].

Digital image processing is a rapidly dynamic field in which new applications and techniques are always introduced in both high quality literatures and modern product advertisements. Digital images suffer from many sources of degradations which unfortunately lead to spatial quality distortions. The spatial degradations blur the object edges and thereby the image resolution is decreased. Thus, digital images captured by low quality cameras will be of poor visual resolution and blurred. These Gaussian blurred images may be due to optical system aberration or camera suffering from out of focus lens. Moreover, any camera moving with respect to the object will lead to blurred image. This motion blurred image is smeared along the direction of relative motion, if the position of the camera sensor changes during the exposure of the camera[5]. Digital image enhancement techniques are interested on getting digital

images look better in a subjective process. Ultimately, the vital concept of enhancement of digital images is to highlight certain features of interest in an image[6].

In fact, an edge is a set of linked pixels which are on the border between two districts. Generally, objects and structures are weak defined due to suffering from blurring effects. Image sharpening has an essential function in image processing. The principal objective of image sharpening is to enhance details which have been blurred, either by mistake or by normal effectiveness of image acquisition method[7].

Conventional approaches for achieving the above goals have employed primarily tools of linear systems. On the other hand, there is a necessity for a powerful nonlinear methodology that can be effectively used in image sharpening. Design of some nonlinear filters is performed by training on ideal and observable image samples which are possessed from an available training assortment. A fundamental problem, which exists in the design of nonlinear filter, is to obtain an adequately great assortment of training examples so as to size up the probabilities of the outputs. Design of unlimited nonlinear filters may demand impossible great search spaces which cannot be reasonably exceeded by any training assortment. Thus, the application of filter constraints represents the key aspect of the design of nonlinear filter. The aperture filter is one of the powerful nonlinear constrained methods that can significantly solve the image blurring problem. Promising results in various applications have been achieved by aperture filters e.g. deblurring, denoising and feature recognition. The main issue of this nonlinear filter lies in designing nonlinear operators statistically. Nonlinear operators can be viewed as estimators of a desired ideal random process which is designed from training the estimate on sets of the ideal and observed training pairs. The training pairs are vectors of observed random variables obtained from the window and the ideal random variable. Unless the length of the training vectors is small, it can become computationally difficult to obtain operators that are sufficiently close to the theoretical optimal. The aperture looks at the observed image through a restricted domain and amplitude. Because the amplitude is restricted, any observed image value that falls above or below this restricted value will be trimmed to the corresponding point on the top or bottom of the aperture, respectively[8].

In this paper, a proposed method for sharpening low-quality QR code images is presented. This is performed by extending the aperture filter technique for document image sharpening that was first introduced in[9]. The success of this method, in sharpening Gaussian blurred document images, opened up the possibility to include the study of motion blurring. Thus, the proposed technique is employed to successfully restore both Gaussian and motion blur QR images. The modified aperture filter presents the utilization of the gradient edge directions instead of the pixel intensities of the input QR code images. Thus, indexing of the patterns is performed due to the local gradients rather than the pixel intensities values. This approach is an attempt to design a computationally inexpensive and memory efficient aperture design. The achieved results prove that the proposed method outperforms not only the aperture filter family but also a number of sharpening filters.

II. OVERVIEW OF THE APERTURE FILTER

The aperture filter is a nonlinear type of operator performed in image processing. The aperture filter is trained by the aid of a training set. The training set is made up of pairs of original and distorted images. At each location, the aperture filter is trained to produce the output to be the most appropriate intensity difference between pixels in the original and the distorted images. This difference value is supposed to be the suitable offset. At each location, by adding the calculated offset to the distorted image pixel it may be fixed to be as near as possible to the original image. At each pixel, the aperture is an orifice which the image can be observed through. Conceptually, this aperture is the product between the domain window and the gray range amplitude of the image values in the domain window. Consequently, each pixel intensity in the domain window is tested such that intensity values less and more than the amplitude range [$-l,l$] of the domain window are mapped to the bottom and top of the aperture respectively. This mapping reduces the probability space of the watched pixel intensity values to a fewer group of variables. Therefore, the grayscale aperture filter is applied under two window restrictions. The window domain [$-d,d$] decides the aperture spatial extent. On the other hand, the amplitude range [$-l,l$] defines the window gray intensities of the aperture.

For a signal Y under observation, where $Y = (y_0, y_1, y_2,\ldots)$, each point, y_j, $-d \le j \le d$, of the original watched signal is projected into the trimmed observation, y_j^*, $-d \le j \le d$ according to the function shown in equation (1).

$$y_j^* = \begin{cases} y_j & -l \le y_j \le l \\ l & y_j > l \\ -l & y_j < -l \end{cases} \qquad (1)$$

The aperture P is the set $(2l+1)$ $(2d+1)$, which is the product between the range [$-l,l$] and the domain [$-d,d$].

The fundamental problem for a pair of signals, Y which is watched and X which is predicted, is to discover a filter F which reduces an error measurement between $F(Y(t))$ and $X(t)$. The output of the aperture filter is predicted by the aid of the conditional probabilities of the true signal assuming the group of watched signal in the filter window is given. The optimal restricted filter is provided by $E[S|Y^*]$ where, S is a prediction of the ideal random signal and Y^* is the trimmed watched signal according to equation (1). In this comprehensive analysis, assume that all signals including the ideal signal S, utilized in this prediction are trimmed inside the masked range [$-l,l$]. Under this prediction, the

optimal restricted filter is introduced by E [$S^*|Y^*$], where S* is the trimmed value of S.

After a couple of years, significant research efforts have been developed to increase the efficiency of the aperture filter. The aperture filter resolution was incremented by altering the positioning of the aperture and adjusting the domain of the window. Instead of placing the aperture on the watched pixel value, it was positioned in the window on the median value of the watched pixels[10]. Furthermore, a grayscale aperture filter using an envelope approach was introduced in[11]. This approach was utilized to overcome the inadequate amount of data in order to sufficiently construct filters with no needs of prior or constraint information. Multimask aperture filters were demonstrated by Green *et al.*[12]. The masks were selected to match patterns which are frequently occurred in the input image. Moreover, Green *et al.*[13] presented a multiresolution aperture filter depending on joining knowledge from various resolutions.

III. DIRECTIONAL APERTURE METHOD

For each pixel, the directional gradient is obtained by using the gradient edge operator. The directional gradient is calculated by applying the first differentiation to the pixel in a definite window. The simplicity in discovering edges and their angular positions is the main advantage of the gradient edge operator. The directional gradient can be obtained by the aid of a number of well-known methods such as: Prewitt, Sobel, Robinson, Kirsch and others[14]. Sobel is the standard against all these edge directions. In the spatial domain, Sobel kernel is convolved with the window of the pixel under test to calculate the directional gradient. The 2 Sobel kernels[15], utilized in the convolution process, are (3x3 mask) or (5x5 mask).

Every spatial pixel *y(i,j)*, the edge vector is described by $H(i,j) = (hx_{i,j}, hy_{i,j})$ where *hxi,j* and *hyi,j* are calculated by applying the 2 convolution kernels *Rx* and *Ry*. The pixel direction is represented by the angle that is calculated according to equation (2).

$$Ang\,(H(i,j)) = (180^o/\pi) \times \arctan(hy_{i,j}/hx_{i,j}) \quad (2)$$

The directional gradient, which is ranging between ($0^o \sim 180^o$), was previously separated into 4 discrete bins. However, other researchers used 8 discrete bins. In this work, the directional gradient is separated into 30 discrete bins. Directional gradient is produced for each spatial pixel by the aid of equation (2), and is placed into the appropriate bin of the 30 discrete bins.

The directional aperture method utilizes (3x3 or 5x5) window in the calculations used in this paper. These window sizes produce an adequate agreement between the training size data set and the achieved accuracy. In the training phase, a two parts algorithm is performed. The goal is achieving a classification for an input image to useful homogeneous classes according to specific features, i.e. directional gradient and neighboring amplitude variations.

First, the directional gradient is calculated and the pixel under test is located in one of the 30 different bins (each bin interval comprises of 6^o). Unfortunately, the calculated directional gradient was solely inadequate to provide the correct offset value to fix the blur effects. Actually, the neighboring pixel amplitude variation can place the directional gradient into several clusters i.e. changing from dark to bright or bright to dark. Thus, the need for a second stage is appeared. For each directional gradient, the groups of pixels with the same neighboring amplitude variations are grouped by the help of a clustering algorithm. A four-dimensional vector *Hz*, comprising the features, is calculated for every pixel *y(i,j)*. Where *Hz* = (*hx1, hx2, hy1, hy2*). The local pixel intensity variation is captured by using this feature vector. *hxl* value is provided by applying the convolution process between only the positive term of the kernel *Rx* and the window of *y(i,j)*. In a similar way, *hx2* is the computed value by applying the convolution process between only the negative term of the kernel *Rx* and the window of *y(i,j)*. In addition, *hy1* and *hy2* are provided by applying the convolution process between the positive as well as the negative terms of the kernel *Ry* and the window of *y(i,j)*, respectively. For a certain directional gradient, the four-dimensional vectors *Hz* are arranged in distinct classes depending on the calculated Euclidean distance.

Thus, a summary of the aforementioned procedures can be presented as follows:

• A window is passed through the whole blurred image Y. For each pixel *y(i,j)*, the directional gradient is calculated and a certain discrete bin is allocated.

• The feature vector *Hz* of each directional gradient is composed from *hx1, hx2, hy1 and hy2*.

• Depending on the feature vector of each pixel in each bin, the classification algorithm is sequentially performed. By calculating the Euclidean distance (E_i) between the incoming feature vector Hz_{new} and the entire feature vectors of the same distinct directional gradient by the aid of equation (3).

$$E_i = \sqrt{\sum_{j=1}^{4} (Hz_{new_j} - Hz_{ij})^2} \qquad i = (1,\ldots,k) \quad (3)$$

Where k is the number of classes in this directional gradient. E_i^* is the minimum Euclidean distance of the winning class i^*.

• If the winning class i* satisfies the following condition:

$E_i^* \leq T$ (where T is a certain threshold)

Then,

The pixel is assigned to the nearest class i^*.

Else,

A new class is considered, which is composed of the incoming feature vector Hz_{new}.

• At the end of the development of the entire training process, the filtering method is constructed. Now, the directional aperture is produced by means of a lookup table which assigns a given offset value to specific classes of input patterns. The value of the offset is the best predicted difference between the referenced and the blurred pixel. After performing the training phase, the value of the offset, which is frequently repeated, will be assigned to the calculated class.

• The directional aperture method can now be utilized to sharpen the incoming blurred QR code image. Once the cluster of a certain directional gradient seen in the incoming blurred QR code image, the enhanced QR code image is sharpened by adding the frequently repeated offset of the winning class according to the built lookup table.

IV. EXPERIMENTAL RESULTS

The proposed aperture filter (PAF) is presented to sharpen blurred QR code images in this section. We apply our algorithm to a number of grayscale QR code images with varying degrees of both Gaussian blur and motion blur. The efficiency of the PAF is evaluated against a group of aperture filter family including, 7 × 7 × 7 conventional aperture filter[8], multimask aperture filter[12] and multiresolution aperture filter[13]. Furthermore, PAF is examined against Niblack's method[16] which is one of the best locally thresholding method.

Fig. 1: (a) Image1. (b) – (f) Image1 distorted with varying degrees of both Gaussian blur and motion blur that are used in the training stage.

Moreover, for Gaussian blur image sharpening, the efficiency of the PAF is assessed against 2 filters: The modified high-pass filter[17], and lower upper middle (LUM) filter[18]. On the other hand, for motion blur image sharpening, the proposed filter is extensively compared with three deconvolution methods: Matlab's blind deconvolution method, Lucy-Richardson method[19] and maximum-a-posteriori (MAP) method[20].

Our algorithm was evaluated on the published dataset[21] which is composed of six grayscale QR code images. The PAF is demonstrated with five experiments. In each experiment, the first image is used in training, while the other five images are used in testing. The used QR code images resolution is 72 pixels per inch (ppi). Besides subjective results, two different quantitative measures: the peak signal to noise ratio (PSNR) and the structural similarity index (SSIM) are utilized to filtering results evaluation. The output of each filter is assessed by comparing its estimation to the original image.

Small Gaussian Blur: As a first experiment, Fig. 1(a) and (b) demonstrate the referenced and the distorted "Image1". The degradation is applied by a 2.0 pixels radius Gaussian blur. The training phase is performed by these two images to later help in the following filtering phase. The first experiment is applied on the five other QR code images. In this experiment, "Image2" is used as an example to present the subjective results. Fig. 2(a) and (b) present blurred "Image2" by a 2.0 pixels radius Gaussian blur and the filtered image after performing PAF. Fig. 7 and Fig. 8 introduce the quantitative evaluation including PSNR and SSIM between the aforementioned sharpening filters for the five distorted images.

Large Gaussian Blur: As a second experiment, Fig. 1(a) and (c) demonstrate the referenced and the distorted "Image1". The degradation is applied by a 3.0 pixels radius Gaussian blur. The training phase is performed by these two images to later help in the following filtering phase. The second experiment is applied on the five other QR code images. In this experiment, "Image3" is used as an example to present the subjective results. Fig. 3(a) and (b) present blurred "Image3" by a 3.0 pixels radius Gaussian blur and the filtered image after performing PAF. Fig. 9 and Fig. 10 introduce the quantitative evaluation including PSNR and SSIM between the aforementioned sharpening filters for the five distorted images. In this experiment, PAF utilizes window sizes 5x5 to measure the local gradient.

Window sizes 3x3 are insufficient due to the large blurring radius.

(a) (b)

Fig. 2: (a) Distorted Image2 by a 2.0 pixels radius Gaussian blur (b) PAF.

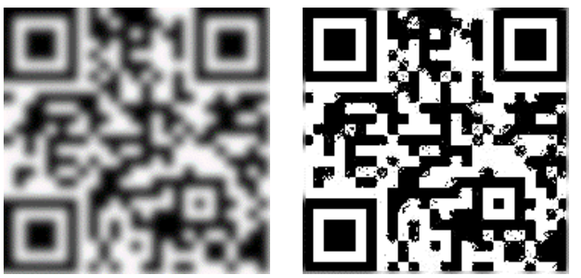

(a) (b)

Fig. 3: (a) Distorted Image3 by a 3.0 pixels radius Gaussian blur (b) PAF.

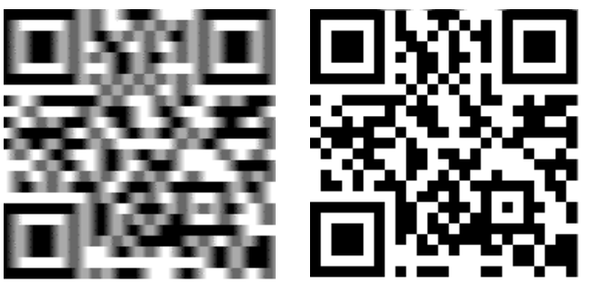

(a) (b)

Fig. 4: (a) Distorted Image4 by a distance of 10 pixels motion blur (b) PAF.

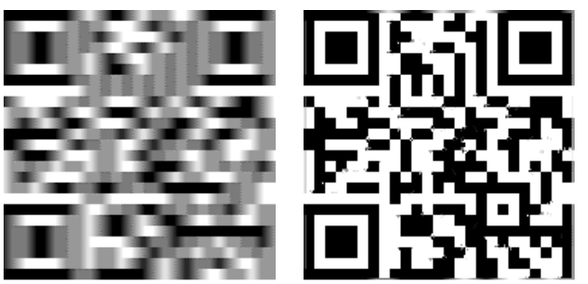

(a) (b)

Fig. 5: (a) Distorted Image5 by a distance of 15 pixels motion blur (b) PAF.

Small Motion Blur: As a third experiment, Fig. 1(a) and (d) demonstrate the referenced and the distorted "Image1". The degradation is applied by a distance of 10 pixels motion blur. The training phase is performed by these two images to later help in the following filtering phase. The third experiment is applied on the five other QR code images. In this experiment, "Image4" is used as an example to present the subjective results. Fig. 4(a) and (b) present blurred "Image4" by a distance of 10 pixels motion blur and the filtered image after performing PAF. Fig. 11 and Fig. 12 introduce the quantitative evaluation including PSNR and SSIM between the aforementioned sharpening filters for the five distorted images.

Large Motion Blur: As a fourth experiment, Fig. 1(a) and (e) demonstrate the referenced and the distorted "Image1". The degradation is applied by a distance of 15 pixels motion blur. The training phase is performed by these two images to later help in the following filtering phase. The fourth experiment is applied on the five other QR code images. In this experiment, "Image5" is used as an example to present the subjective results. Fig. 5(a) and (b) present blurred "Image5" by a distance of 15 pixels motion blur and the filtered image after performing PAF. Fig. 13 and Fig. 14 introduce the quantitative evaluation including PSNR and SSIM between the aforementioned sharpening filters for the five distorted images. In this experiment, PAF utilizes window sizes 5x5 to measure the local gradient. Window sizes 3x3 are insufficient due to the large distance of the motion blur.

Small Gaussian Blur and Small Motion Blur: As a fifth experiment, Fig. 1(a) and (f) demonstrate the referenced and the distorted "Image1". The degradation is applied by a 2.0 pixels radius Gaussian blur followed by a distance of 10 pixels motion blur. The training phase is performed by these two images to later help in the following filtering phase. The fifth experiment is applied on the five other QR code images. In this experiment, "Image6" is used as an example to present the subjective results. Fig. 6(a) and (b) present blurred "Image6" by a 2.0 pixels radius Gaussian blur followed by a distance of 10 pixels motion blur and the filtered image after performing PAF. Fig. 15 and Fig. 16 introduce the quantitative evaluation including PSNR and SSIM between the aforementioned sharpening filters for the five distorted images.

From the visual filtered images, the curves of PSNR and SSIM following Gaussian and motion blur a number conclusions is provided. Comparisons of the filtered images obviously indicate that the PAFs achieve a significant major improvement in many aspects including both fine details and edges restoration. From the PSNR and SSIM graphs, it is evident that the proposed filters have lower PSNR and higher SSIM all over the tested images. Experimental results prove that the efficiency of the PAFs is better than that of many other well-known aperture-types and sharpener filters as well.

V. CONCLUSION

Nowadays, handheld and wearable devices can access web pages by the aid of QR codes. The QR code information can be decoded to many URLs relating to the original image, and more information corresponding to the original image can be reached by the consumers, such as online shopping and much more. Spatial degradation of object edges causes blurring and thereby the QR code image loses resolution. This is mainly caused by the capture device being out of focus or being accidently moving during the scanning process. Nonlinear filters have been discovered to give a significant improvement over other linear methods in many aspects of image deblurring. Aperture methodology is a successful nonlinear filter that can powerfully solve the image blurring problem. A proposed aperture filter is designed which is mainly focused on sharpening QR code images. The improvement according to QR code image enhancement and error calculation was verified against other aperture-type filter designs as well as other well-known sharpening techniques. Experimental results demonstrate that the proposed directional gradient aperture filter improved both the visibility and the perceptibility of various structures in blurred QR images. Thus, our enhancement algorithm brings blurred QR scanning one step nearer to enterprise-grade performance and provides an affordable opportunity to enhance not only the practical applicability but also the consumer shopping experiences.

(a) (b)

Fig. 6: (a) Distorted Image6 by a 2.0 pixels radius Gaussian blur followed by a distance of 10 pixels motion blur (b) PAF.

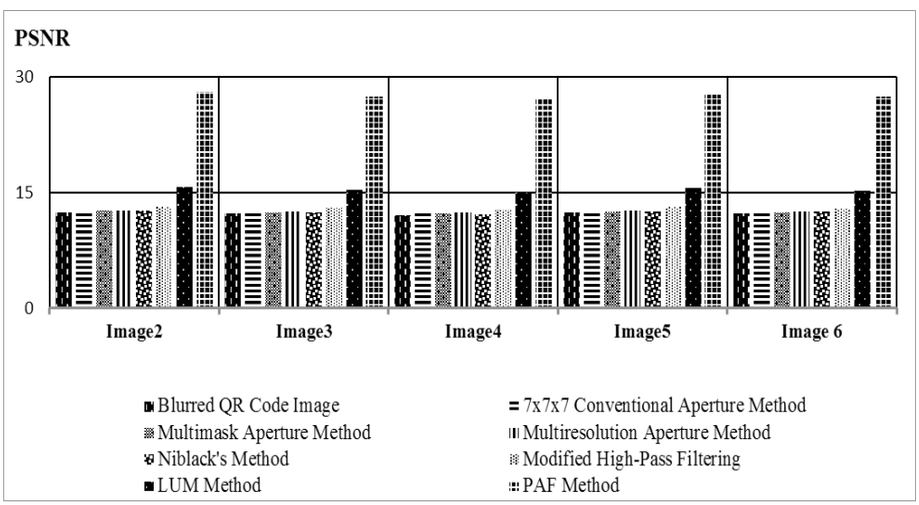

Fig. 7: PSNR for different sharpener-type filters applied on distorted QR code images blurred by a 2.0 pixels radius Gaussian blur.

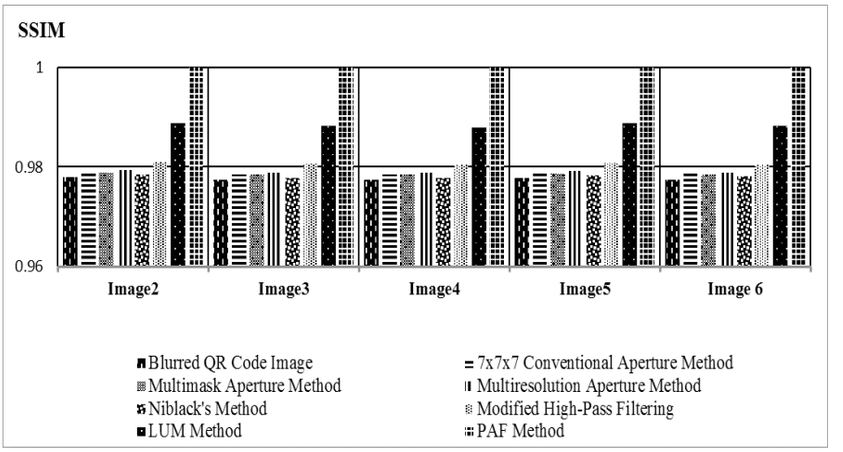

Fig. 8: SSIM for different sharpener-type filters applied on distorted QR code images blurred by a 2.0 pixels radius Gaussian blur.

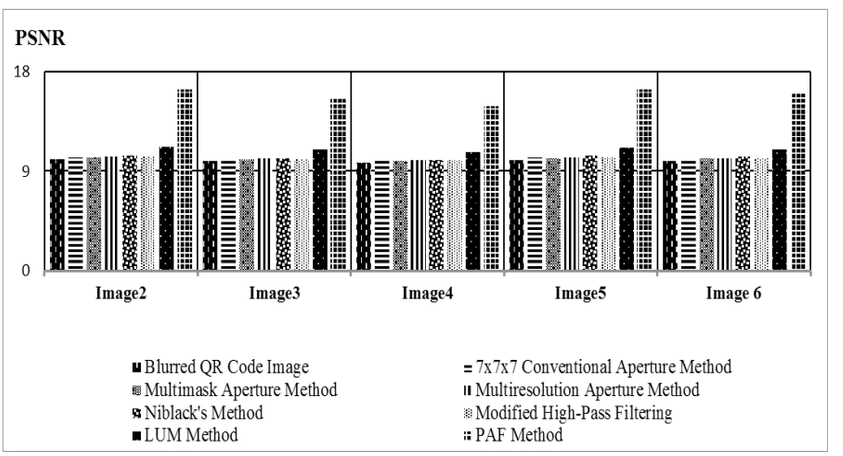

Fig. 9: PSNR for different sharpener-type filters applied on distorted QR code images blurred by a 3.0 pixels radius Gaussian blur

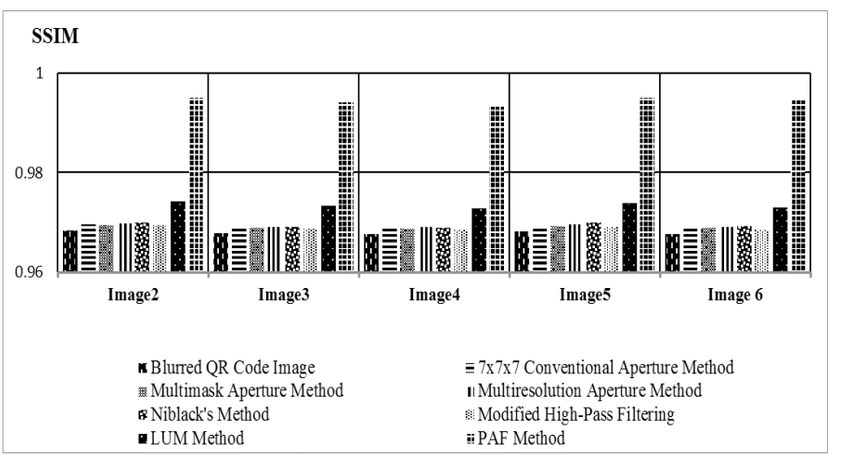

Fig. 10: SSIM for different sharpener-type filters applied on distorted QR code images blurred by a 3.0 pixels radius Gaussian blur.

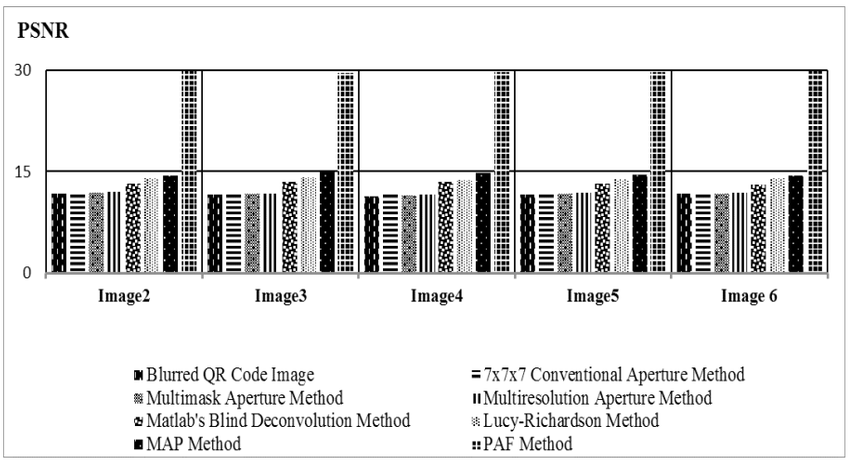

Fig. 11: PSNR for different sharpener-type filters applied on distorted QR code images blurred by a distance of 10 pixels motion blur.

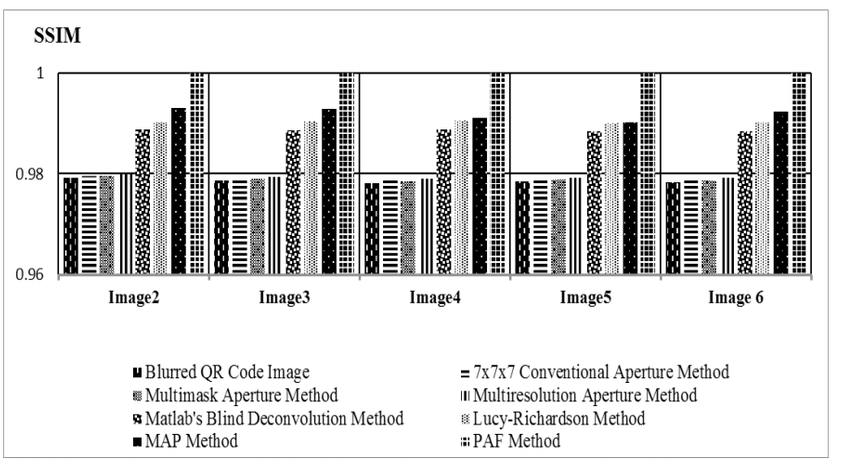

Fig. 12: SSIM for different sharpener-type filters applied on distorted QR code images blurred by a distance of 10 pixels motion blur.

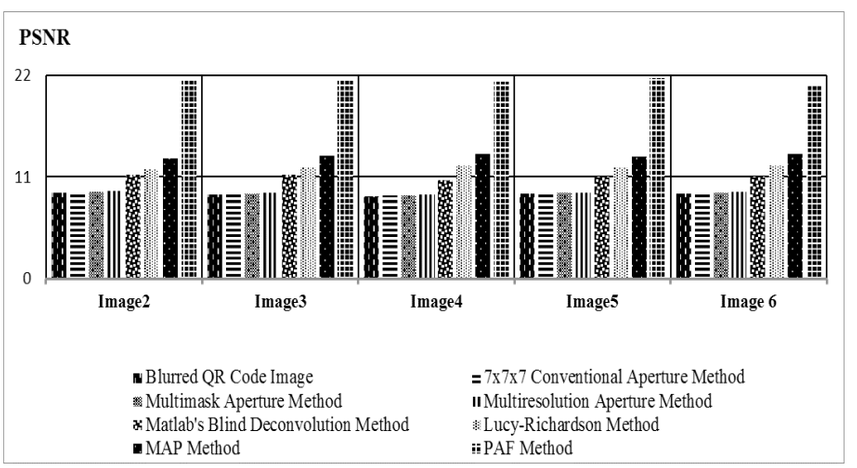

Fig. 13: PSNR for different sharpener-type filters applied on distorted QR code images blurred by a distance of 15 pixels motion blur.

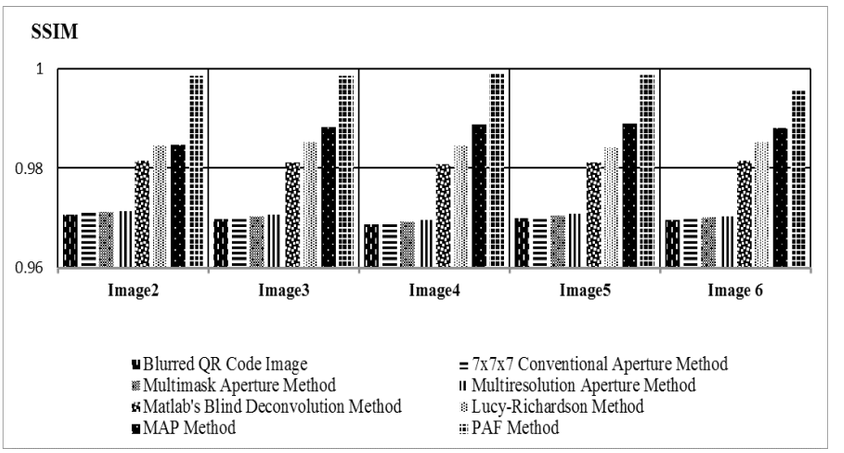

Fig. 14: SSIM for different sharpener-type filters applied on distorted QR code images blurred by a distance of 15 pixels motion blur.

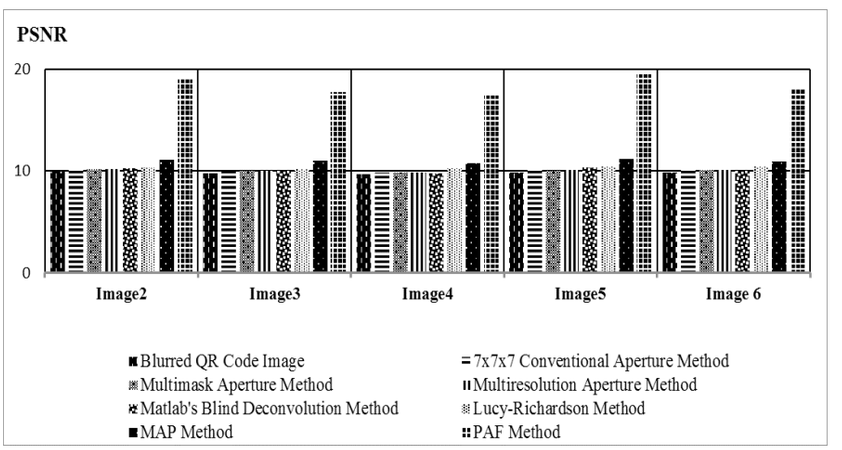

Fig. 15: PSNR for different sharpener-type filters applied on distorted QR code images blurred by a 2.0 pixels radius Gaussian blur followed by a distance of 10 pixels motion blur

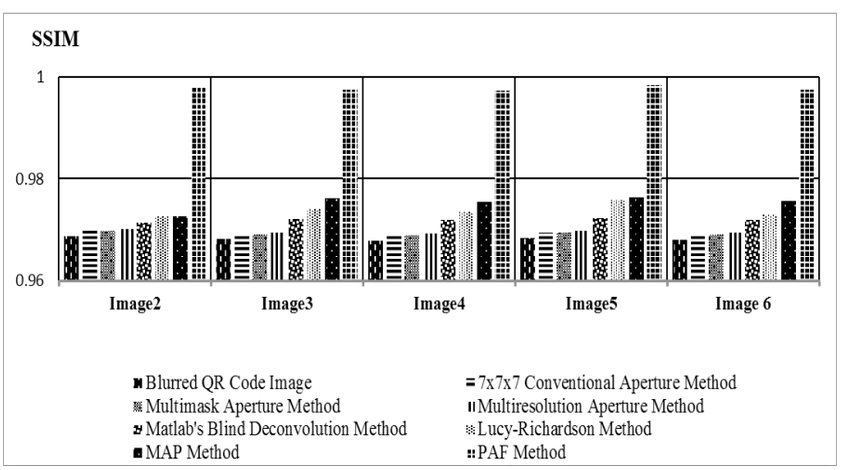

Fig. 16: SSIM for different sharpener-type filters applied on distorted QR code images blurred by a 2.0 pixels radius Gaussian blur followed by a distance of 10 pixels motion blur

VI. REFERENCES

[1] D. Munoz-Mejias, I. Gonzalez-Diaz and F. Diaz-de-Maria, "A low-complexity pre-processing system for restoring low-quality QR code images," IEEE Trans. Consum. Electron., vol. 57, no. 3, pp. 1320-1328, 2011.
[2] G. Soros, S. Semmler, L. Humair and O. Hilliges, "Fast blur removal for wearable QR code scanners," in Proc. ISWC, Osaka, Japan, Sept. 7-11, 2015.
[3] Z. Cui, *et al*., "Supporting web-based visualization through ad hoc computational clusters of mobile devices," Inform Visual., vol. 18, no. 2, pp. 195-210, 2019.
[4] Y. Lin, Y. Chang and J. Wu, "Appearance-based QR code beautifier," IEEE Trans. Multimedia, vol. 15, no. 8, pp. 2198-2207, 2013.
[5] M. Abbass, *et al*., "Image deconvolution using homomorphic technique,"SIViP, vol. 13, no. 4, pp. 703-709, 2019.
[6] Y. Gennip, P. Athavale, J. Gilles and R. Choksi, "A regularization approach to blind deblurring and denoising of QR barcodes," IEEE Trans. Image Process., vol. 24, no. 9, pp. 2864-2873, 2015.
[7] R. Gonzalez and R. Woods, Digital Image Processing. 4th ed., Upper Saddle River, NY, USA: Pearson, Prentice Hall, 2018.
[8] Jr., Hirata, E. Dougherty and J. Barrera, "Aperture filters," Signal Process., vol. 80, no. 4, pp. 697-721, 2000.
[9] T. Mahmoud and S. Marshall, "Document image sharpening using a new extension of the aperture filter," SIViP, vol. 3, no. 4, pp. 403-419, 2009.
[10] Jr., Hirata, J. Barrera and E. Dougherty, "Design of grey-scale nonlinear filters via multiresolution apertures," in Proc. EUSIPCO, Tampere, Finland, Sept. 4-8, 2000.
[11] M. Brun, Jr., Hirata, J. Barrera and E. Dougherty, "Nonlinear filter design using envelopes," J. of Math. Imag. and Vision, vol. 21, no. 1, pp. 81-97, 2004.
[12] A. Green, S. Marshall, D. Greenhalgh, E. Dougherty, "Design of multi-mask aperture filters," Signal Process., vol. 83, no. 9, pp. 1961-1971, 2003.
[13] A. Green, E. Dougherty, S. Marshall and D. Greenhalgh, "Optimal filters with multiresolution apertures," J. of Math. Imag. and Vision, vol. 20, no. 3, pp. 237-250, 2004.
[14] M. Sharifi, M. Fathy and M. Mahmoudi, "A classified and comparative study of edge detection algorithms," in Proc. ITCC, Las Vegas, Nevada, USA, Apr. 8-10, 2002.
[15] J. Russ and F. Neal, The Image Processing Handbook. Boca Raton, Florida, USA: CRC Press, Taylor & Francis Group, 2016.
[16] W. Niblack, An Introduction to Digital Image Processing. Englewood Cliffs, New Jersey, USA: Prentice Hall, 1986.
[17] M. Fischer, J. Paredes and G. Arce, "Weighted median image sharpeners for the world wide web," IEEE Trans. Image Process., vol. 11, no. 7, pp. 717–727, 2002.
[18] R. Hardie and C. Boncelet, "LUM filters: a class of rank-order-based filters for smoothing and sharpening," IEEE Trans. Signal Process, vol. 41, no. 3, pp. 1061–1076, 1993.
[19] W. Richardson, "Bayesian-based iterative method of image restoration," J. of the Opt. Soc. of Amer., vol. A 62, pp. 55-59, 1972.
[20] J. Kotera, F. Sroubek and P. Milanfar, "Blind deconvolution using alternating maximum a posteriori estimation with heavy-tailed priors," in: R. Wilson, E. Hancock, A. Bors and W. Smith "Computer analysis of images and patterns (CAIP)," Lecture Notes in Computer Science, 8048, Springer, Berlin, Heidelberg, 2013.
[21] QReate and Track, [Online]. Available: http://qreateandtrack.com/qr-code-examples-and-ideas, (accessed 15 December 2019).